

## Article

# Asymmetric Synthesis of Enantiomerically Pure Aliphatic and Aromatic D-Amino Acids Catalyzed by Transaminase from *Haliscomenobacter hydrossis*

Alina K. Bakunova, Tatiana Y. Isaikina, Vladimir O. Popov and Ekaterina Yu. Bezsudnova \* 

Bach Institute of Biochemistry, Research Centre of Biotechnology of the Russian Academy of Sciences, Leninsky Ave. 33, Bld. 2, Moscow 119071, Russia

\* Correspondence: eubez@inbi.ras.ru

**Abstract:** D-amino acids are valuable building blocks for the synthesis of biologically active compounds and pharmaceuticals. The asymmetric synthesis of chiral amino acids from prochiral ketones using stereoselective enzymes is a well-known but far from exhausted approach for large-scale production. Herein, we investigated a pyridoxal-5'-phosphate-dependent D-amino acid transaminase from *Haliscomenobacter hydrossis* as a potential biocatalyst for the enzymatic asymmetric synthesis of optically pure aliphatic and aromatic D-amino acids. We studied the catalytic efficiency and stereoselectivity of transaminase from *H. hydrossis* in the amination of aliphatic and aromatic  $\alpha$ -keto acids, using D-glutamate as a source of the amino group. We constructed a one-pot three-enzyme system, which included transaminase and two auxiliary enzymes, hydroxyglutarate dehydrogenase, and glucose dehydrogenase, to produce D-amino acids with a product yield of 95–99% and an enantiomeric excess of more than 99%. We estimated the stability of the transaminase and the cofactor leakage under reaction conditions. It was found that a high concentration of  $\alpha$ -keto acids as well as a low reaction temperature (30 °C) can reduce the cofactor leakage under reaction conditions. The obtained results demonstrated the efficiency of transaminase from *H. hydrossis* in the asymmetric synthesis of enantiomerically pure D-amino acids.

**Keywords:** D-amino acid transaminase; substrate specificity; synthesis of D-amino acids; stereoselective amination of keto acids; PLP leakage



**Citation:** Bakunova, A.K.; Isaikina, T.Y.; Popov, V.O.; Bezsudnova, E.Y. Asymmetric Synthesis of Enantiomerically Pure Aliphatic and Aromatic D-Amino Acids Catalyzed by Transaminase from *Haliscomenobacter hydrossis*. *Catalysts* **2022**, *12*, 1551. <https://doi.org/10.3390/catal12121551>

Academic Editors: Katarzyna Wińska, Antoni Szumny and Wanda Mączka

Received: 1 November 2022

Accepted: 25 November 2022

Published: 1 December 2022

**Publisher's Note:** MDPI stays neutral with regard to jurisdictional claims in published maps and institutional affiliations.



**Copyright:** © 2022 by the authors. Licensee MDPI, Basel, Switzerland. This article is an open access article distributed under the terms and conditions of the Creative Commons Attribution (CC BY) license (<https://creativecommons.org/licenses/by/4.0/>).

## 1. Introduction

In the modern world, the use of enzymes as catalysts provides many valuable benefits, including mild reaction conditions with high enantioselectivity, conversion, and high yield [1,2]. Biocatalysis has proven to be an environmentally friendly alternative to chemical synthesis [2,3]. Enzyme applications in the large-scale industrial production of various chemicals have proven particularly advantageous in obtaining optically pure substances [1,3,4]. Among optically active compounds, chiral amines are of great importance in the agrochemical and pharmaceutical industries [5–7]. Amines and amino compounds account for up to 90% of the top-selling or approved small molecular drugs, and around 30% of pesticides are chiral amine molecules [3].

D-amino acid biocatalytic production is under intense scrutiny because of the growing interest in pharmaceuticals containing nonproteinogenic D-amino acids [8,9]. Since D-amino acids are frequently detected in the natural antibiotics isolated from microorganisms, invertebrates, and amphibians, they can be used as a basis for the development of medicinal and veterinary antimicrobial agents. Moreover, among the peptides containing D-amino acids in the organisms, there are not only peptidoglycans and antibiotics but also neuropeptides, hormones, hepatotoxins, opioid peptides, etc. [8].

Currently, amino acid production is based on microbial fermentation and, to a lesser extent, on enzymatic synthesis [10,11]. Advances in fermentation technology and strain im-

provement of amino acid-producing microorganisms raised fermentation to a predominant industrial-scale production technique for L-amino acids [10,12]. D-amino acids are obtained mainly as by-products of resolution in L-amino acid production [10]. Over the years, several enzymes that produce or metabolize D-amino acids have been discovered, and enzymatic synthesis of D-amino acids has been suggested accordingly [13]. These are D-hydantoinases and D-carbamoylases, D-amino acid aminotransferases, N-acyl-D-amino acid amidohydrolases, D-amino acid dehydrogenases, etc., as well as amino acid oxidases and acylases for enzymatic resolution [13–15]. Unfortunately, the enzymatic approaches suffer from various drawbacks, including specific substrate requirements, unfavorable equilibrium, low reaction rate, etc. [10,13]. Cascade multi-enzyme processes significantly improved the effectiveness of enzymatic synthesis of D-amino acids [16–21] due to the desired equilibrium shift and simplification of the starting reactants. D-amino acid aminotransferases (DAAT, EC 2.6.1.21) are among the key enzymes of enzymatic cascade systems [15,17], and they catalyze stereoselective amination of  $\alpha$ -keto acids. DAATs belong to pyridoxal-5'-phosphate (PLP)-dependent transaminases of fold type IV and catalyze the reversible stereoselective transfer of an amino group from D-amino acid (amino donor) to  $\alpha$ -keto acid (amino acceptor), producing new D-amino acid and  $\alpha$ -keto acid [22–24]. According to extensive studies, various non-proteinogenic D-amino acids and their keto analogs are among DAAT substrates [25–28]. In the cell, DAATs are commonly known to synthesize D-glutamate for cell wall peptidoglycans [8,12]. Other D-amino acids are synthesized in the cell through racemization or epimerization processes catalyzed by various racemases and NRP epimerization domains [12]. Successful examples of transaminase engineering [29–31] raised the industrial potential of DAATs in the synthesis of unnatural products.

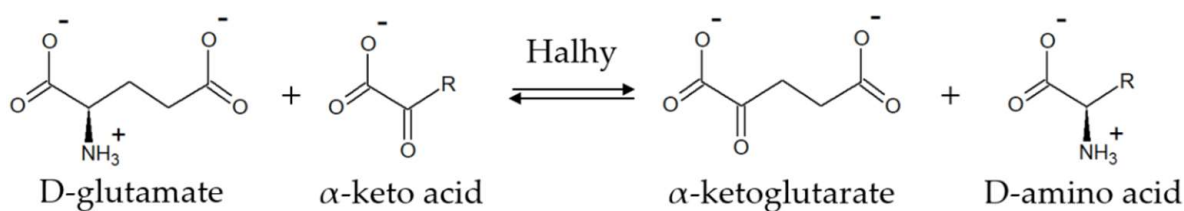
Previously, we reported the purification and biochemical and structural characterization of a new DAAT from the bacterium *Haliscomenobacter hydrossis* (Halhy) [32]. Substrate specificity analysis revealed a wide substrate scope of Halhy, which included aromatic and aliphatic  $\alpha$ -keto acids, D-alanine, D-leucine, and D-glutamate. Halhy was not active toward primary amines and L-amino acids. The steady-state kinetic analysis showed that  $\alpha$ -ketoglutarate and pyruvate were the best substrates for Halhy, and the highest rate was achieved in the reaction between D-glutamate and pyruvate in K-phosphate buffer, pH 8.0, at 40 °C. The activity of Halhy remained unchanged at 40 °C for four days and decreased to 40% in one day at 50 °C. We obtained the crystal structure of the holo form of Halhy (PDB ID 7P7X) and performed a detailed structural analysis of the active site with the identification of functional residues involved in substrate binding.

In this work, the applicability of DAAT from *H. hydrossis* (Halhy) to stereoselective amination of various  $\alpha$ -keto acids was investigated. Considering the high activity of Halhy toward various aliphatic and aromatic  $\alpha$ -keto acids as well as its high thermostability at 40–50 °C, we examined the catalytic efficiency of Halhy in transamination reactions between D-glutamate and various  $\alpha$ -keto acids; we analyzed the enantioselectivity and product yield; we estimated the stability of Halhy and the cofactor leakage under reaction conditions. The results encouraged us to suggest Halhy for the enzymatic asymmetric synthesis of enantiomerically pure aliphatic and aromatic D-amino acids.

## 2. Results

### 2.1. $\alpha$ -Keto Acid Substrate Scope of Halhy

Halhy was tested in the overall transamination reaction with various aromatic and aliphatic  $\alpha$ -keto acids and 4 mM D-glutamate as an amino donor in 50 mM K-phosphate buffer, pH 8.0, at 40 °C (Scheme 1).



**Scheme 1.** Transamination reaction between D-glutamate and  $\alpha$ -keto acid catalyzed by Halhy.

These are optimal reaction conditions for Halhy [32]. The steady-state kinetic parameters are shown in Table 1. Halhy demonstrated significant activity toward all but one of the tested  $\alpha$ -keto acids. The highest rate was achieved in the reaction between D-glutamate and pyruvate. In reactions with aliphatic  $\alpha$ -keto acids, the values of the maximal velocity as well as the specificity constant ( $k_{cat}/K_m$ ) values decrease as the substrate side chain was lengthened; moreover, the specificity constants for the branched-chain  $\alpha$ -keto acids with a methyl substituent at  $C_\beta$  atom were lower than those for the linear ones. No activity was observed in the reaction with trimethylpyruvate, which has three methyl substituents at the  $C_\beta$  atom. The third methyl group at the  $C_\beta$  atom appeared to cause steric hindrance near the  $C_\alpha$  atom of the substrate, thus preventing the transamination reaction. The specificity constants for the aromatic  $\alpha$ -keto acids were higher than those for the aliphatic ones with a C6 chain length. Apparently, the aromaticity improved the binding of the substrate to the enzyme. Among the aromatic substrates, the highest activity was observed in the reaction between D-glutamate and phenylpyruvate, as well as D-glutamate and 4-hydroxyphenylpyruvate. Thus, Halhy effectively converted various hydrophobic  $\alpha$ -keto acids. No substrate inhibition was observed in the examined  $\alpha$ -keto acid concentration ranges (see Supplementary Materials).

**Table 1.** Steady-state kinetic parameters of the overall transamination reaction between D-glutamate and various  $\alpha$ -keto acids catalyzed by Halhy in 50 mM K-phosphate buffer, pH 8.0, at 40 °C.

Substrate	Structure	Corresponding Amino Acid	$V_{max}$ , U/mg	$k_{cat}$ , s <sup>-1</sup>	$K_m$ , mM	$k_{cat}/K_m$ , s <sup>-1</sup> M <sup>-1</sup>
pyruvate		D-alanine	380 ± 10	215 ± 6 *	2.1 ± 0.1 *	103,000 ± 8000 *
2-oxobutyrate		D-homoalanine	71 ± 1	40.0 ± 0.6	1.6 ± 0.1	25,000 ± 2000
2-oxovalerate		D-norvaline	48 ± 4	27 ± 2	13.5 ± 0.3	2000 ± 200
3-methyl-2-oxobutyrate		D-valine	46 ± 2	26 ± 1	18 ± 2	1400 ± 200

Table 1. Cont.

Substrate	Structure	Corresponding Amino Acid	$V_{max}$ , U/mg	$k_{cat}$ , s <sup>-1</sup>	$K_m$ , mM	$k_{cat}/K_m$ , s <sup>-1</sup> M <sup>-1</sup>
2-oxohexanoate		D-norleucine	4.6 ± 0.4	2.6 ± 0.2	43 ± 5	60 ± 10
3-methyl-2-oxovalerate		D-isoleucine	17.6 ± 0.4	10 ± 0.2	200 ± 50	50 ± 20
4-methyl-2-oxovalerate		D-leucine	35 ± 2	20 ± 1	110 ± 6	200 ± 10
trimethylpyruvate		D-tert-leucine		ND		
phenylpyruvate		D-phenylalanine	35 ± 2	20 ± 1	36 ± 3	560 ± 70
indol-3-pyruvate		D-tryptophan	3.7 ± 0.2	2.1 ± 0.1	5.0 ± 0.2	420 ± 40
4-hydroxyphenylpyruvate		D-tyrosine	34 ± 2	19 ± 1	8 ± 1	2400 ± 400
2-oxo-4-phenylbutyrate		D-homophenylalanine	6.7 ± 0.4	3.8 ± 0.2	16.0 ± 0.8	240 ± 20

\*—from [32]; ND—not detected.

## 2.2. Cofactor Leakage under Reaction Conditions

The stability of the holo form of a transaminase (PLP form and PMP form) significantly affects the product yield of the catalytic reaction, since the dissociation of the cofactor generates an inactive and often unstable apo form of the enzyme. Usually, a small amount of free PLP is added to the reaction mixture to shift the equilibrium toward the holo form of the transaminase [25–28]. To investigate the stability of the Halhy PLP form under reaction conditions (substrates, 50 mM K-phosphate buffer, pH 8.0, at 30–40 °C), the PLP leakage was analyzed by evaluating changes in the concentration of the Halhy PLP form spectrophotometrically by the absorbance decay at 450 nm. The wavelength was chosen to minimize the contribution of the unbound PLP to the absorbance (Figure 1). It should be noted that the PLP conversion into the PMP form induced the absorbance changes at 450 nm as well (Figure 1). Incubation of the Halhy PLP form with substrates (10 mM  $\alpha$ -ketoglutarate and 100 mM D-alanine) was accompanied by the absorbance decay at 450 nm, thus indicating a decrease in the concentration of the PLP form of Halhy (Figure 2A, curve 1). The desalting of the reaction mixture after 40 min of incubation revealed the complete dissociation of the cofactor from the enzyme active site and the presence of the apo form of Halhy in the solution (Figure 2B); the observed rate constant of the PLP dissociation under these conditions was  $0.048 \pm 0.006 \text{ min}^{-1}$ .

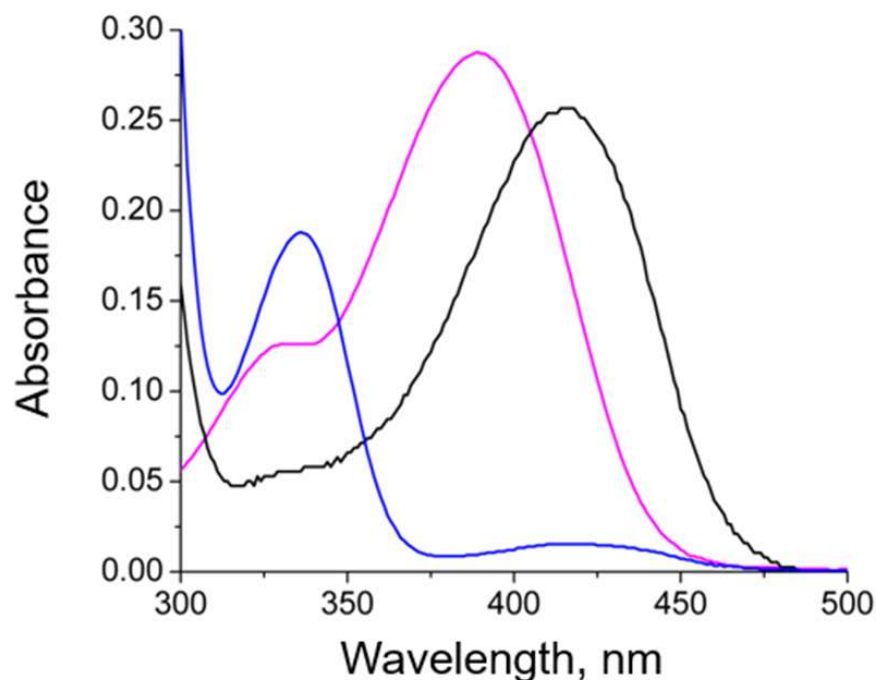


**Figure 1.** Absorbance spectra of the Halhy PLP form (black) at a concentration of 1 mg/mL, the Halhy PMP form (blue) at a concentration of 1 mg/mL, and 30  $\mu\text{M}$  PLP (magenta) in 50 mM K-phosphate buffer, pH 8.0, at 25 °C.

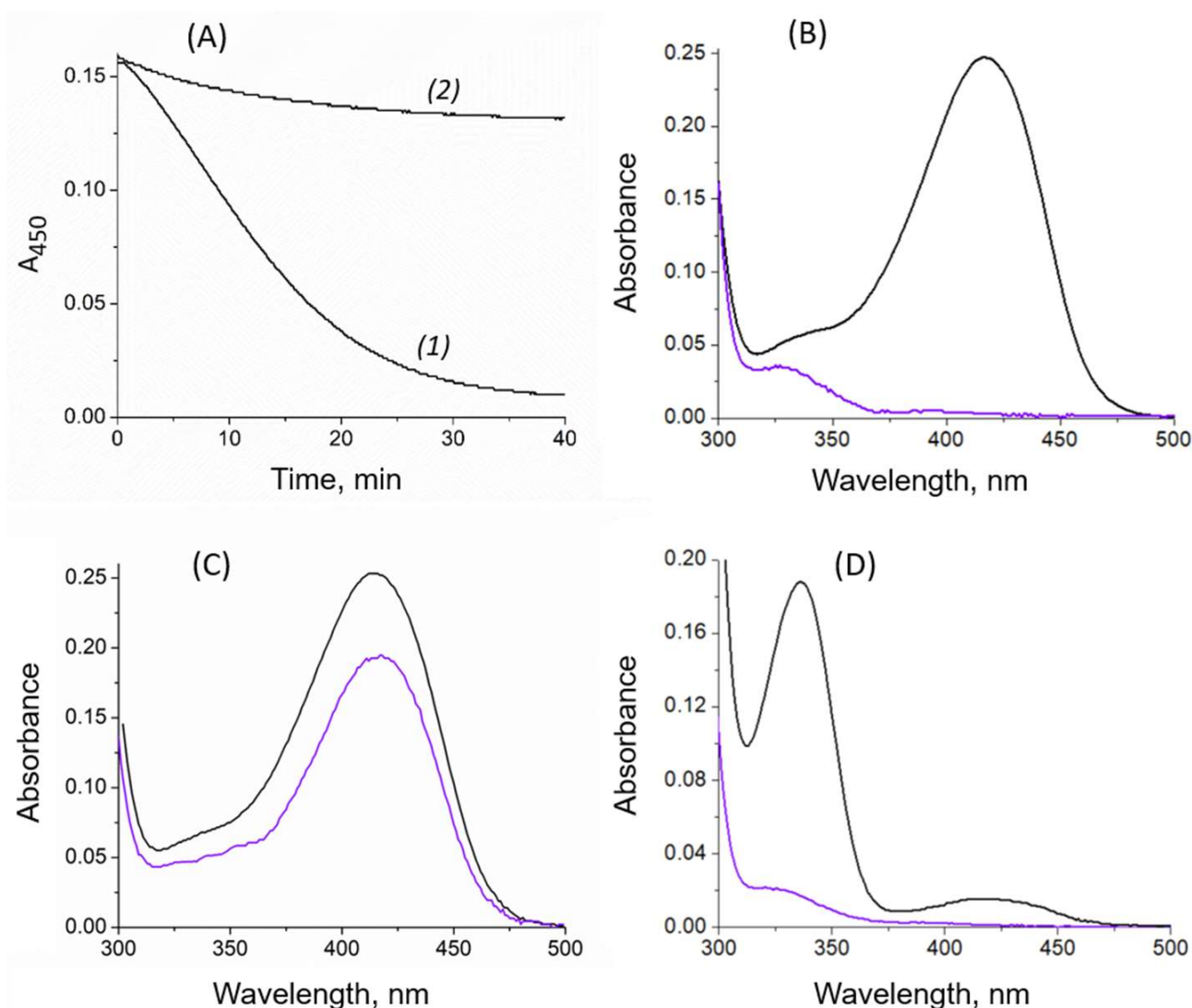
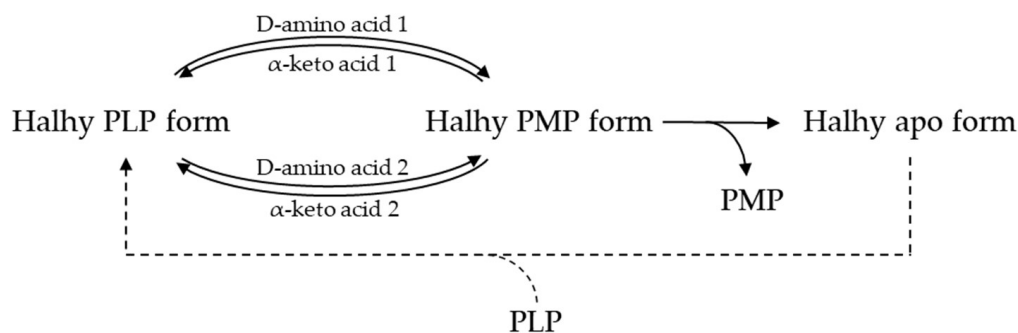


**Figure 2.** Cofactor leakage under reaction conditions in 50 mM K-phosphate buffer, pH 8.0, at 40 °C. (A) Absorbance change with time for the PLP form of Halhy (1.2 mg/mL) in the presence of 10 mM  $\alpha$ -ketoglutarate and 100 mM D-alanine (curve 1) and in buffer (curve 2). (B) Absorption spectra of the PLP form of Halhy before (black) and after 40 min of incubation with 10 mM  $\alpha$ -ketoglutarate and 100 mM D-alanine followed by desalting (purple). (C) Absorption spectra of the PLP form of Halhy before (black) and after 40 min of incubation in buffer followed by desalting (purple). (D) Absorption spectra of the PMP form of Halhy before (black) and after 40 min of incubation in buffer followed by desalting (purple).

For comparison, in 50 mM K-phosphate buffer at 40 °C without substrates, the observed rate constant of the PLP dissociation was only  $0.012 \pm 0.001 \text{ min}^{-1}$  (Figure 2A, curve 2), and the desalting after 40 min incubation confirmed the partial dissociation of the cofactor (Figure 2C). When the PMP form of Halhy (the absorbance maximum of the PMP form of Halhy was observed at 337 nm) was incubated alone in 50 mM K-phosphate buffer at 40 °C, the desalting confirmed the complete loss of PMP (Figure 2D) as well, with the observed rate constant of the PMP dissociation being  $0.156 \pm 0.012 \text{ min}^{-1}$ , which was much higher than the observed rate constant of the PLP dissociation from the holo form (with or without substrates). Apparently, PMP is weakly bound in the active site of Halhy. Thus, leakage of the cofactor under operational conditions (with substrates) appears to proceed via the PMP formation followed by the PMP dissociation (Scheme 2).



**Scheme 2.** Proposed mechanism of cofactor leakage under reaction conditions.

We estimated the effects of  $\alpha$ -keto acid concentrations, temperature, and the extra PLP on the rate of PLP leakage (Figure 3) and calculated the half-life of the PLP form of Halhy under various reaction conditions (Table 2). Lowering the temperature to 30 °C increased the half-life of the PLP form of Halhy from 10 to 50 min (Figure 3A). The excess of  $\alpha$ -keto acid concentration (amino acceptor, which is active with PMP) relative to the amino donor (D-alanine or D-glutamate) concentration had a significant impact on the half-life of the PLP form of Halhy. The change in the (amino acceptor):(amino donor) concentration ratio from 1:10 to 1:1 (Figure 3B) gave a three-times increase in the half-life. The half-life of the PLP form of Halhy in the presence of 50 mM  $\alpha$ -ketoglutarate and 50 mM D-alanine was 170 min, in the presence of 50 mM 2-oxoalverate and 50 mM D-glutamate—240 min. It is interesting that the addition of 100  $\mu$ M PLP to the reaction mixture with 10 mM  $\alpha$ -ketoglutarate and 100 mM D-alanine resulted only in a slight stabilization of the Halhy PLP form; the half-life changed from 50 to 62 min at 30 °C and from 10 to 17 min at 40 °C. Overall, Halhy in the PLP form is preferable under operational conditions due to the high rate of leakage of the cofactor in the PMP form. The percentage of the Halhy PLP form can be significantly increased by lowering the temperature and increasing the concentration of  $\alpha$ -keto acids (amino acceptor).

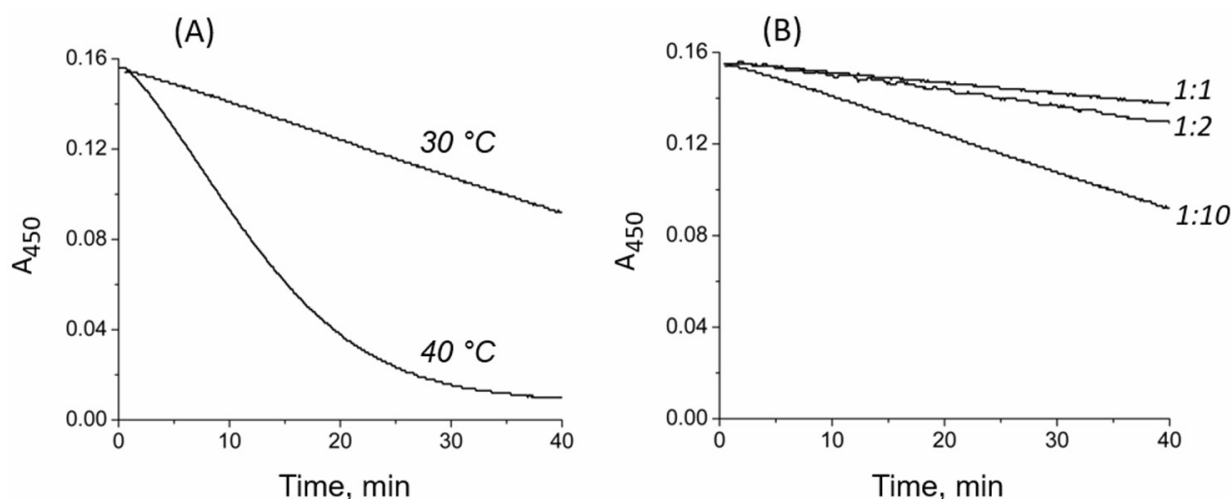


**Figure 3.** Effects of temperature and  $\alpha$ -keto acid concentration on the PLP leakage from the PLP form of Halhy (1.2 mg/mL) under reaction conditions. (A) Time-dependence of the absorbance of the Halhy PLP form in the presence of 10 mM  $\alpha$ -ketoglutarate and 100 mM D-alanine in 50 mM K-phosphate buffer, pH 8.0, at 30 and 40 °C. (B) Time-dependence of the absorbance of the Halhy PLP form in the presence of substrates at different concentration ratios: 10 mM  $\alpha$ -ketoglutarate and 100 mM D-alanine (1:10), 50 mM  $\alpha$ -ketoglutarate and 100 mM D-alanine (1:2), 50 mM  $\alpha$ -ketoglutarate and 50 mM D-alanine (1:1) in 50 mM K-phosphate buffer, pH 8.0, at 30 °C.

**Table 2.** Half-life of the PLP form of Halhy under various reaction conditions.

Reaction Conditions				$k_{\text{diss}}^{\text{app}}, \text{min}^{-1}$	Half-Life, min
Amino Donor	Amino Acceptor	Temperature, °C	[PLP], $\mu\text{M}$		
100 mM D-alanine	10 mM $\alpha$ -ketoglutarate	40	0	$0.048 \pm 0.006$	$10 \pm 1$
100 mM D-alanine	10 mM $\alpha$ -ketoglutarate	40	100	$0.030 \pm 0.004$	$17 \pm 2$
100 mM D-alanine	10 mM $\alpha$ -ketoglutarate	30	0	$0.010 \pm 0.001$	$50 \pm 5$
100 mM D-alanine	10 mM $\alpha$ -ketoglutarate	30	100	$0.008 \pm 0.002$	$62 \pm 15$
100 mM D-alanine	50 mM $\alpha$ -ketoglutarate	30	0	$0.005 \pm 0.001$	$100 \pm 20$
50 mM D-alanine	50 mM $\alpha$ -ketoglutarate	30	0	$0.0030 \pm 0.0003$	$170 \pm 20$
50 mM D-glutamate	50 mM 2-oxovalerate	30	0	$0.0021 \pm 0.0003$	$240 \pm 30$

### 2.3. Asymmetric Synthesis of D-Amino Acids

To evaluate the feasibility of Halhy as a biocatalyst, we examined the product yield and enantiomeric excess of D-amino acids in the reactions catalyzed by Halhy. D-glutamate was used as the amino donor. To shift the equilibrium of the transamination reaction to the products, a one-pot three-enzyme system was applied. The  $\alpha$ -ketoglutarate formed in the transamination reaction was converted to (*R*)-2-hydroxyglutarate using NAD-dependent (*R*)-2-hydroxyglutarate dehydrogenase (HGDH) [33]. The consumed NADH was regenerated in the D-glucose oxidation reaction catalyzed by glucose dehydrogenase (GDH) (Scheme 3). The formation of hydroxyglutarate, together with the recycling of NADH and the non-enzymatic hydrolysis of D-glucono-1,5-lactone, shifted the equilibrium toward the formation of D-amino acids. The process was performed at 30 °C, at an (amino acceptor):(amino donor) concentration ratio of 1:1, and with the addition of 100  $\mu\text{M}$  PLP. The post-mixing concentrations of D-glutamate and  $\alpha$ -keto acids were 50 mM, accordingly. The amination process continued for 72 h, and finally product yield and enantiomeric excess were determined (Table 3, Figure S2). The product yield exceeded 90% for most  $\alpha$ -keto acids, and the enantiomeric excess of the obtained D-amino acids exceeded 99%.

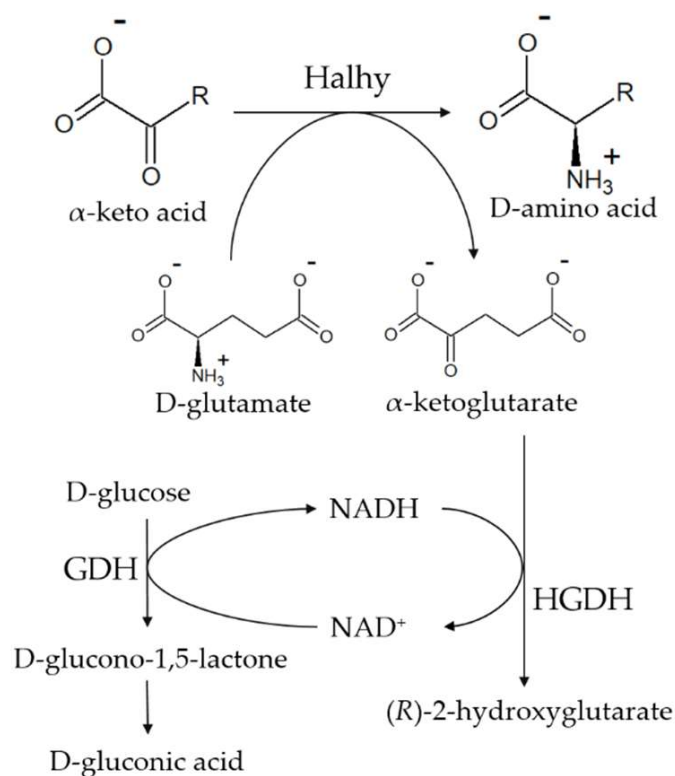
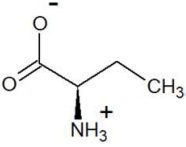
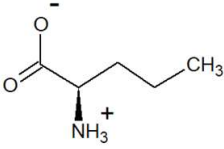
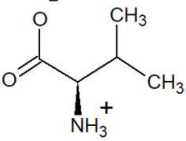
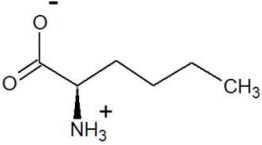
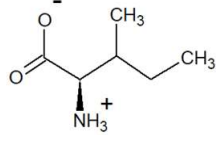
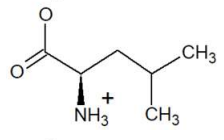
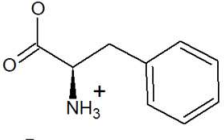
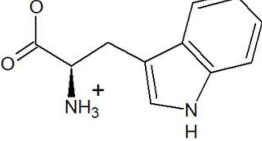
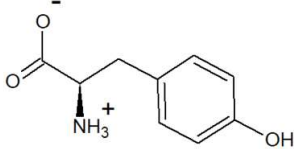
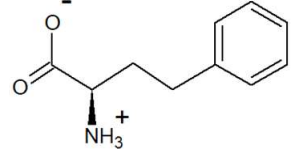
**Scheme 3.** One-pot three-enzyme system to produce D-amino acids.

Table 3. Asymmetric synthesis of D-amino acids.

Substrate	Product	Product Yield, %	ee, %
2-oxobutyrate	D-homoalanine 	99	>99.5
2-oxovalerate	D-norvaline 	95.7	>99.3
3-methyl-2-oxobutyrate	D-valine 	99	>99
2-oxohexanoate	D-norleucine 	99	>99
3-methyl-2-oxovalerate	D-isoleucine 	90	>99
4-methyl-2-oxovalerate	D-leucine 	98.5 *	>99.4 *
phenylpyruvate	D-phenylalanine 	95.6 *	>99.3 *
indol-3-pyruvate	D-tryptophan 	75 **	>99.6
4-hydroxyphenylpyruvate	D-tyrosine 	85	>99.7
2-oxo-4-phenylbutyrate	D-homophenylalanine 	99	>99.1

\*—from [32]; \*\*—Synthesis of D-tryptophan was carried out at a post-mixing concentration of indol-3-pyruvate of 10 mM because of the high rate of the non-enzymatic oxidation of indol-3-pyruvate in water [34].

We also analyzed the yield of 2-oxovalerate and 2-oxo-4-phenylbutyrate amination product with the shortening of the synthesis time. After 17 h, the product yield reached 98% (*ee* > 99%) and 99% (*ee* > 99%) for D-norvaline and D-homophenylalanine, respectively. In addition, we investigated the effectiveness of Halhy in the amination process at high substrate loading. After 17 h of the reaction between 500 mM 2-oxo-valerate and 500 mM D-glutamate, the product yield reached 73%, and after 17 h of reaction between 500 mM 2-oxo-4-phenylbutyrate and 500 mM D-glutamate, the product yield was only 33%; the product yield remained unchanged for the next 55 h. Thus, high concentrations of substrates reduced the product yield of the  $\alpha$ -keto acid amination. The inactivation of enzymes, Halhy, HGDH, or GDH, was not excluded.

We assessed the stability of Halhy under operational conditions with two pairs of substrates: D-glutamate and 2-oxovalerate, and D-glutamate and phenylpyruvate (Figure 4). The half-life of Halhy in the presence of 2-oxovalerate and D-glutamate was around four days, and in the presence of phenylpyruvate and D-glutamate, only one day. Thus, the aromatic substrate induced a higher rate of irreversible denaturation of Halhy. The observed half-life of Halhy was much longer than that of the PLP form of Halhy (Table 2). In other words, the apoenzyme retained the ability to bind the cofactor and regenerate the active PLP form for a long time.

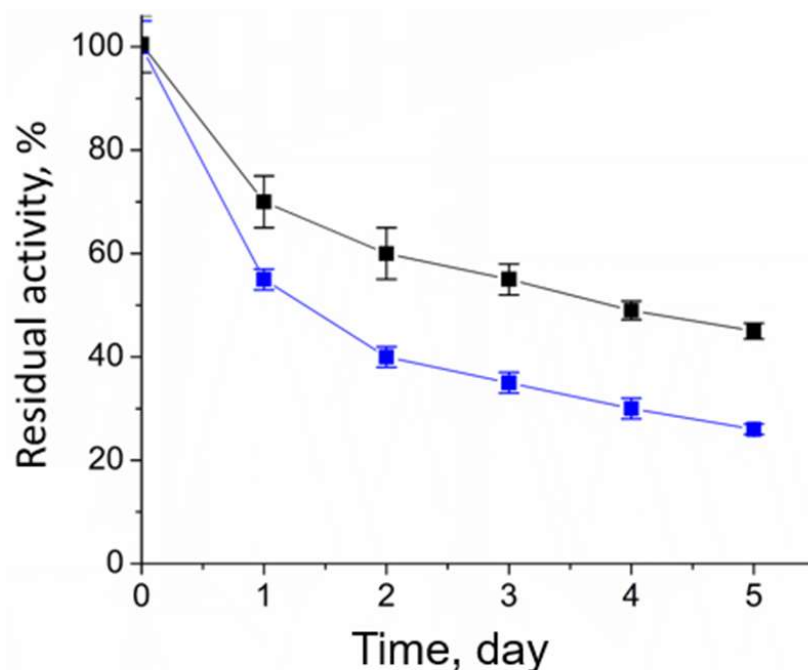


**Figure 4.** Operational stability of Halhy. The time-dependence of the residual activity of Halhy under the asymmetric synthesis conditions: 1 mg/mL Halhy, 50 mM 2-oxovalerate (black) or phenylpyruvate (blue), 50 mM D-glutamate, 100  $\mu$ M PLP, 1 mM NADH, 150 mM D-glucose in 100 mM K-phosphate buffer, pH 7.5, at 30 °C; 100% corresponds to  $200 \pm 10$  U/mg in the standard assay. Error bars represent standard deviation.

Overall, Halhy is effective in the stereoselective amination of  $\alpha$ -keto acids at 30 °C. The 500 mM of substrates is not fatal to Halhy. High operational stability, effective regeneration of the PLP form of the enzyme, and high rates of transamination reactions are clear advantages of Halhy for industrial applications. The obtained results showed the potential applicability of Halhy in the asymmetric synthesis of D-amino acids.

### 3. Discussion

The high stereospecificity of DAATs makes them excellent biocatalysts for stereoselective amination of  $\alpha$ -keto acids. Most of the currently proposed cascade processes for the synthesis of D-amino acids include DAAT from the genus *Bacillus* at the stage of transamination [16–21]. The well-studied DAAT from *Bacillus* sp. YM-1 is a thermostable enzyme, active over a wide temperature range from 30 to 60 °C [17,25,35,36]. This DAAT and its homologs from the genus *Bacillus* were applied in the asymmetric synthesis of substituted D-tryptophans [18], various hydrophobic amino acids, including D-homoalanine, D-valine, D-leucine, D-phenylalanine, and D-tyrosine at 35–37 °C [17,19–21]. The enantiomeric excess in D-amino acids exceeded 99% [17]. The achieved specific activities of these DAATs toward aliphatic and aromatic  $\alpha$ -keto acids varied between 0.2 and 2.0 U/mg at 35 °C [17]. D-amino acid transaminase from *H. hydrossis* catalyzed transamination reactions with much higher rates; the maximal velocity in the reaction between D-glutamate and pyruvate achieved 380 U/mg at 40 °C. The rates of asymmetric synthesis of D-amino acids, catalyzed by Halhy, varied from 3.7 U/mg in the indol-3-pyruvate conversion to 71 U/mg for the 2-oxobutyrate conversion in 50 mM K-phosphate buffer, pH 8.0, at 40 °C. The enantiomeric excesses of D-amino acids in the studied processes exceeded 99% both for aromatic and aliphatic substrates. Further studies on the development of cascade processes in which a low-cost amino group donor could be used instead of D-glutamate are promising. The usage of isopropylamine as an amino donor requires active site engineering, since naturally Halhy does not react with isopropylamine. At the same time, based on the obtained results, a four-enzyme cascade catalytic system can be developed, with D-glutamate generated in situ by L-glutamate dehydrogenase and glutamate racemase from ammonium ion and  $\alpha$ -ketoglutarate, with the addition of formate dehydrogenase for NADH recycling [21].

PLP-dependent transaminase applications do not require the auxiliary cofactor regeneration process. According to the mechanism, PLP converts into the PMP form in the first half reaction with an amino donor and then regenerates to the PLP form in the second half reaction with an amino acceptor, thus completing the overall transamination reaction cycle [22,23]. However, the PMP form of transaminase suffers from the leakage of PMP [37,38]. While the cofactor in the PLP form is bound in the active site both by electrostatic interactions of its phosphate group and by Schiff-base linkage with the catalytic lysine, the PMP form of the cofactor is stabilized only by electrostatic interactions; this explains the lower stability of the PMP forms of some transaminases compared to their PLP forms. It should be noted that PLP also dissociates from the active site due to hydrolysis of the Schiff-base linkage, but to a lesser extent [37]. Usually, a small amount of PLP (1–50  $\mu$ M) is added both to the storage buffer and the reaction mixture [25–28] to shift the equilibrium toward a holo form. In this work, we analyzed the cofactor leakage from the Halhy holo form under reaction conditions that differ from the storage conditions by the presence of substrates. We found significant cofactor leakage under reaction conditions at 40 °C. During the catalytic act, the unstable PMP form of the enzyme was generated. We succeeded in significant reduction of the cofactor leakage by lowering the temperature of the reaction and increasing the  $\alpha$ -keto acid concentration. As a result, the efficiency of converting PMP to PLP exceeded the efficiency of the PMP dissociation from the active site, thereby retaining the cofactor in the active site. In addition, according to the operational stability experiments, Halhy was found to be resistant to irreversible denaturation under reaction conditions; the residual activity was around 50% after four days at 30 °C. These data refer to the stability of the protein globule of Halhy (apoenzyme). The effective approaches to the holo form stabilization together with the high stability of the Halhy apo form are quite beneficial for industrial applications. According to the achieved results, Halhy can be suggested as an effective biocatalyst for the asymmetric synthesis of aliphatic and aromatic D-amino acids.

## 4. Materials and Methods

### 4.1. Expression and Purification of Recombinant Halhy

The expression and purification of Halhy have been described in detail in [32]. Briefly, the His6TEV-tagged Halhy was expressed in *E. coli* BL21(DE3)pLys (Novagen, Darmstadt, Germany). The recombinant Halhy was isolated using Ni-affinity chromatography. Fractions showing the activity were stored in 50 mM K-phosphate buffer, pH 8.0, containing 100 mM NaCl, 300  $\mu$ M PLP, and 50% glycerol at  $-20$  °C.

The (*R*)-2-hydroxyglutarate dehydrogenase (HGDG) from *Acidaminococcus fermentans* was produced and purified similarly. The purified enzyme was desalted in 100 mM K-phosphate buffer, pH 8, and stored at  $-20$  °C in 50% glycerol.

The amino acid sequences were checked by MALDI-TOF MS analysis (UltraFLEXtreme Bruker Daltonik, Bremen, Germany).

### 4.2. Enzyme Activity Assay

The activity of Halhy in the overall transamination reaction with different  $\alpha$ -keto acids was determined using a coupled enzyme assay with HGDH to detect a  $\alpha$ -ketoglutarate production [33]. The reaction mixture contained 50 mM K-phosphate buffer, pH 8; 30  $\mu$ M PLP; 4 mM D-glutamate; 1–150 mM  $\alpha$ -keto acid; 0.01–10  $\mu$ M of the purified Halhy; 330  $\mu$ M NADH; and 4 U/mL HGDH at 40 °C. The reaction was initiated by  $\alpha$ -keto acid after pre-incubation of the enzyme in the reaction mixture without  $\alpha$ -keto acid for 10 min at 40 °C. The reaction progress was monitored spectrophotometrically by a decrease in the absorbance ( $\epsilon_{\text{NADH}} = 6220 \text{ M}^{-1} \text{ cm}^{-1}$ ) at 340 nm, using a SPECTROstar Omega (BMG Labtech GmbH, Ortenberg, Germany). The reaction progress with indol-3-pyruvate or 4-hydroxyphenylpyruvate was monitored at 450 nm ( $\epsilon_{\text{NADH}} = 3000 \text{ M}^{-1} \text{ cm}^{-1}$ ) because of the high absorption of these substances at 340 nm.

The activity of Halhy was calculated from the initial linear region of the progress curve of the reaction. One unit (U) was defined as the amount of the enzyme that catalyzed the conversion of 1  $\mu$ mol of the substrate into a product per minute. Steady-state kinetic parameters of the reactions were determined from the substrate saturation curves at the constant co-substrate concentration. Saturation curves were analyzed using the Michaelis–Menten model. The kinetic parameters were calculated by fitting the initial velocity data to Equation (1):

$$V = \frac{V_{max} \times [A] \times [B]}{K_M^A \times [B] + K_M^B \times [A] + [A] \times [B]} \quad (1)$$

where  $V$  is the initial velocity,  $V_{max}$  is the maximal velocity,  $A$  and  $B$  are substrate concentrations, and  $K_M^A$  and  $K_M^B$  are the Michaelis constants of substrates  $A$  and  $B$ , respectively. All measurements were performed at least in triplicate. The data were analyzed using Origin 8.0 software (OriginLab, Northampton, MA, USA, 2009).

### 4.3. Cofactor Leakage Assay

The PLP form of Halhy was obtained by incubating Halhy with 10 molar excess of PLP and 20 mM  $\alpha$ -ketoglutarate for 30 min at 25 °C, followed by the transfer into 50 mM K-phosphate buffer, pH 8.0, using a HiTrap desalting column (Cytiva, Marlborough, MA, USA). The PMP form of Halhy was obtained by incubating the PLP form of Halhy with 500 mM D-alanine for 30 min at 25 °C, followed by the transfer into 50 mM K-phosphate buffer, pH 8.0. The process of PLP dissociation from the Halhy PLP form was monitored by the decay of absorbance at 450 nm, using the UV–Vis spectrophotometer Evolution 300 equipped with a Peltier cell (Thermo Scientific, Waltham, MA, USA). The process of PMP dissociation from the Halhy PMP form was monitored by the decay of absorbance at 337 nm. The Halhy PLP form (or the Halhy PMP form) at a concentration of 1.3 mg/mL (36  $\mu$ M) was incubated in 50 mM K-phosphate buffer, pH 8.0, or in the reaction mixture at

30 and 40 °C. The apparent PLP (or PMP) dissociation rate constant was calculated from a linear part (3–5 min) of the observed absorbance decrease using the following Equation (2):

$$k_{\text{diss}}^{\text{app}} = -\frac{1}{A_0} \times \frac{dA}{dt} \quad (2)$$

where  $A_0$  is the absorbance at  $t = 0$ . The value of half-life time (see Supplementary Materials) was estimated as

$$t_{1/2} = \frac{1}{k_{\text{diss}}^{\text{app}}} \times \frac{1}{2}. \quad (3)$$

#### 4.4. Enzymatic Synthesis of D-Amino Acids

The reaction mixture contained 50 mM D-glutamate, 50 mM keto acid, 100  $\mu$ M PLP, 1 mg/mL Halhy, 1 mM NADH, 150 mM D-glucose, 90 U/mL HGDH, and 50 U/mL glucose dehydrogenase (Sigma, St. Louis, MO, USA) in 100 mM K-phosphate buffer, pH 7.5. The reaction mixtures were incubated for 3 days at 30 °C. The reaction mixtures with a high substrate load contained 500 mM D-glutamate, 500 mM  $\alpha$ -keto acid, 100  $\mu$ M PLP, 1 mg/mL Halhy, 1 mM NADH, 1 M D-glucose, 90 U/mL HGDH, and 50 U/mL GDH in 100 mM K-phosphate buffer, pH 7.5. In reaction with 2-oxo-4-phenylbutyrate 20% (*v/v*), DMSO was added to the reaction mixture because of the low solubility of  $\alpha$ -keto acid.

#### Analysis of the Product Yield and the Enantiomeric Excess of D-Amino Acids

The product yield was determined by analyzing the consumption of  $\alpha$ -keto acids or the production of D-amino acids by HPLC assay. The low molecular weight fractions were separated from the reaction mixtures using Amicon-Ultra-15 centrifugal tubes (Millipore, Burlington, MA, USA). D-tyrosine and D-homophenylalanine precipitates were produced during the reaction. For their dissolving, 20  $\mu$ L of 12 M HCl was added to 500  $\mu$ L of the reaction mixture, and the denatured proteins were removed by centrifugation. The  $\alpha$ -keto acid and D-amino acid concentrations in the aliquots were analyzed by Acta Purifier (Cytiva, Marlborough, MA, USA) equipped with a reverse-phase C18 column (Zorbax Eclipse XDB-C18, 5  $\mu$ m, 4.6 mm  $\times$  150 mm, (Agilent Technologies, Inc., Santa Clara, CA, USA)) at 1.0 mL/min at 25 °C (Appendix A, Table A1).

The enantiomeric excesses of the produced D-amino acids were determined by HPLC assay using a reverse-phase C18 column (Appendix B, Tables A2 and A3). Deproteinized samples were derivatized with Marfey's reagent (Sigma, St. Louis, MO, USA).

#### 4.5. Analysis of the Operational Stability of Halhy

The operational stability of Halhy was analyzed by incubating 1 mg/mL (29.4  $\mu$ M) Halhy in 100 mM K-phosphate buffer, pH 7.5, supplemented with 100  $\mu$ M PLP, 50 mM D-glutamate, 50 mM  $\alpha$ -keto acid, 1 mM NADH, and 150 mM D-glucose at 30 °C. The residual activity of Halhy was determined at regular time intervals in the standard assay: 0.05  $\mu$ g/mL Halhy, 100 mM D-alanine, 10 mM  $\alpha$ -ketoglutarate, 30  $\mu$ M PLP, 330  $\mu$ M NADH, and 2 U/mL lactate dehydrogenase from rabbit muscle (Sigma, St. Louis, MO, USA) in 50 mM K-phosphate buffer, pH 8.0, at 40 °C. The reaction was initiated by  $\alpha$ -ketoglutarate after pre-incubation of the enzyme in the reaction mixture without  $\alpha$ -ketoglutarate for 10 min at 40 °C. The reaction progress was monitored by the decay of absorbance at 340 nm ( $\epsilon_{\text{NADH}} = 6220 \text{ M}^{-1} \text{ cm}^{-1}$ ) using SPECTROstar Omega. The activity of Halhy was calculated from the initial linear region of the progress curve. One unit (U) was defined as the amount of the enzyme that catalyzed the conversion of 1  $\mu$ mol of the substrate into a product per minute.

## 5. Conclusions

We investigated the catalytic efficiency and stereoselectivity of D-amino acid transaminase from *H. hydrossis* in the amination of aliphatic and aromatic  $\alpha$ -keto acids. We analyzed cofactor leakage under reaction conditions and identified two factors that support a high percentage of the more stable PLP form of the enzyme, namely, the excess of  $\alpha$ -keto acid, as well as a low temperature (30 °C). We constructed a one-pot three-enzyme system, which included transaminase from *H. hydrossis* and two auxiliary enzymes, hydroxyglutarate dehydrogenase and glucose dehydrogenase, to produce D-amino acids via stereoselective amination of  $\alpha$ -keto acids at 30 °C using D-glutamate as the source of the amino group. The enantiomeric excess of the target D-amino acids exceeded 99%, and the yield achieved 95–99%. Only with indol-3-pyruvate and 4-hydroxyphenylpyruvate were the yields of the corresponding D-amino acids limited to 75 and 85%, accordingly. The obtained results encouraged us to suggest Halhy for the asymmetric synthesis of D-amino acids.

**Supplementary Materials:** The following supporting information can be downloaded at: <https://www.mdpi.com/article/10.3390/catal12121551/s1>, Figure S1: Steady-state kinetics of the transamination reactions catalyzed by Halhy; Figure S2: HPLC analysis of the enantiomeric excess of D-amino acids after derivatization with Marfey's reagent; The half-life time calculation ( $t_{1/2}$ ).

**Author Contributions:** Conceptualization, A.K.B. and E.Y.B.; Methodology, E.Y.B.; Software, A.K.B.; Validation, A.K.B. and T.Y.I.; Formal Analysis, E.Y.B.; Investigation, A.K.B. and T.Y.I.; Resources, A.K.B. and T.Y.I.; Data Curation, E.Y.B.; Writing—Original Draft Preparation, A.K.B.; Writing—Review and Editing, A.K.B., V.O.P. and E.Y.B.; Visualization, A.K.B.; Supervision, V.O.P.; Project Administration, E.Y.B. and V.O.P.; Funding Acquisition, V.O.P. and E.Y.B. All authors have read and agreed to the published version of the manuscript.

**Funding:** This research was funded by the Russian Science Foundation, grant number 19-14-00164 (in part of steady-state kinetics and asymmetric synthesis data), and the Ministry of Science and Higher Education of the Russian Federation (in part operational stability analysis).

**Data Availability Statement:** The data presented in this study are available in the article or Supplementary Materials.

**Acknowledgments:** The MALDI-TOF MS analysis was carried out using the equipment of the Shared-Access Equipment Centre “Industrial Biotechnology” of the Federal Research Center “Fundamentals of Biotechnology”, Russian Academy of Sciences.

**Conflicts of Interest:** The authors declare no conflict of interest.

## Appendix A

**Table A1.** HPLC analysis conditions.

Compound	Eluent	UV Detection	Retention Time, min
2-oxobutyrate	20 mM NaH <sub>2</sub> PO <sub>4</sub> , pH 2.2, 5% methanol	210 nm	3.0
2-oxovalerate	20 mM NaH <sub>2</sub> PO <sub>4</sub> , pH 2.2, 5% methanol	210 nm	7.4
3-methyl-2-oxobutyrate	20 mM NaH <sub>2</sub> PO <sub>4</sub> , pH 2.2, 5% methanol	210 nm	6.1
2-oxohexanoate	20 mM NaH <sub>2</sub> PO <sub>4</sub> , pH 3.0, 15% methanol	210 nm	5.8
3-methyl-2-oxovalerate	20 mM NaH <sub>2</sub> PO <sub>4</sub> , pH 2.2, 5% methanol	210 nm	15.7
D-tryptophan	20 mM NaH <sub>2</sub> PO <sub>4</sub> , pH 3.0, 15% methanol	280 nm	6.2
D-tyrosine	20 mM NaH <sub>2</sub> PO <sub>4</sub> , pH 2.2, 5% methanol	280 nm	3.9
2-oxo-4-phenyl-butyric acid	20 mM NaH <sub>2</sub> PO <sub>4</sub> , pH 3.0, 30% methanol	210 nm	9.5

## Appendix B

The enantiomeric excess of products was determined by HPLC equipped with a UV detector set at 340 nm using a reverse-phase C18 column. Deproteinized samples were derivatized with Marfey's reagent (Sigma, St. Louis, MO, USA) according to Pavkov-Keller et al. [39]. Briefly, 25  $\mu$ L of Marfey's reagent (28 mM in acetonitrile) and 10  $\mu$ L 1 M

NaHCO<sub>3</sub> were added to a 10 µL sample and incubated at 50 °C for 2 h. The reaction mixture was cooled, and then the reaction was stopped by adding 3 µL of 4 M HCl and 10 µL of 100% methanol.

**Table A2.** HPLC analysis conditions.

Instrument	ÄKTA Purifier, Cytiva, Marlborough, MA, USA
Column	Zorbax Eclipse XDB-C18, 5 µM, 4.6 mm × 150 mm, Agilent Technologies, Inc., Santa Clara, CA, USA
Buffer A	0.1% trifluoroacetic acid in water
Buffer B	0.1% trifluoroacetic acid in 100% methanol
Elution	linear gradient of Buffer B from 20 to 70% in 15 min
Flow rate	1.0 mL/min
Temperature	25 °C
Injection volume	10 µL
Detection	UV, 340 nm

**Table A3.** Retention times of isomers of amino acids after derivatization with Marfey's reagent. HPLC analysis conditions are shown in Table A2.

Compound	RT, min	
	L-isomer	D-isomer
norvaline	16.0	18.6
valine	16.5	19.4
norleucine	17.8	22.0
isoleucine	17.6	21.6
leucine	17.4	20.8
phenylalanine	17.1	20.0
tryptophan	16.0	17.7
tyrosine	20.0	29.0
homophenylalanine	20.1	26.3
homoalanine *	19.2	21.7

\*—linear gradient of Buffer B from 10% to 70% in 20 min.

## References

- Bell, E.L.; Finnigan, W.; France, S.P.; Green, A.P.; Hayes, M.A.; Hepworth, L.J.; Lovelock, S.L.; Niikura, H.; Osuna, S.; Romero, E.; et al. Biocatalysis. *Nat. Rev. Methods Prim.* **2021**, *1*, 46. [CrossRef]
- Winkler, C.K.; Schrittwieser, J.H.; Kroutil, W. Power of Biocatalysis for Organic Synthesis. *ACS Cent. Sci.* **2021**, *7*, 55–71. [CrossRef] [PubMed]
- Wu, S.; Snajdrova, R.; Moore, J.C.; Baldenius, K.; Bornscheuer, U.T. Biocatalysis: Enzymatic Synthesis for Industrial Applications. *Angew. Chem. Int. Ed.* **2021**, *60*, 88–119. [CrossRef]
- Bornscheuer, U.T. The Fourth Wave of Biocatalysis Is Approaching. *Philos. Trans. R. Soc. A Math. Phys. Eng. Sci.* **2018**, *376*, 20170063. [CrossRef] [PubMed]
- Patel, R. Biocatalytic Synthesis of Chiral Alcohols and Amino Acids for Development of Pharmaceuticals. *Biomolecules* **2013**, *3*, 741–777. [CrossRef]
- Brundiek, H.; Höhne, M. Transaminases—A Biosynthetic Route for Chiral Amines. In *Applied Biocatalysis: From Fundamental Science to Industrial Applications*; Wiley-VCH Verlag GmbH & Co. KGaA: Weinheim, Germany, 2016; pp. 199–218, ISBN 9783527677122.
- Zawodny, W.; Montgomery, S.L. Evolving New Chemistry: Biocatalysis for the Synthesis of Amine-Containing Pharmaceuticals. *Catalysts* **2022**, *12*, 595. [CrossRef]
- Grishin, D.V.; Zhdanov, D.D.; Pokrovskaya, M.V.; Sokolov, N.N. D-Amino Acids in Nature, Agriculture and Biomedicine. *Front. Life Sci.* **2020**, *13*, 11–22. [CrossRef]
- Gao, X.; Ma, Q.; Zhu, H. Distribution, Industrial Applications, and Enzymatic Synthesis of d-Amino Acids. *Appl. Microbiol. Biotechnol.* **2015**, *99*, 3341–3349. [CrossRef]
- Leuchtenberger, W.; Huthmacher, K.; Drauz, K. Biotechnological Production of Amino Acids and Derivatives: Current Status and Prospects. *Appl. Microbiol. Biotechnol.* **2005**, *69*, 1–8. [CrossRef]
- Ivanov, K.; Stoimenova, A.; Obreshkova, D.; Saso, L. Biotechnology in the Production of Pharmaceutical Industry Ingredients: Amino Acids. *Biotechnol. Biotechnol. Equip.* **2013**, *27*, 3620–3626. [CrossRef]

12. Radkov, A.D.; Moe, L.A. Bacterial Synthesis of D-Amino Acids. *Appl. Microbiol. Biotechnol.* **2014**, *98*, 5363–5374. [[CrossRef](#)] [[PubMed](#)]
13. Pollegioni, L.; Rosini, E.; Molla, G. Advances in Enzymatic Synthesis of D-Amino Acids. *Int. J. Mol. Sci.* **2020**, *21*, 3206. [[CrossRef](#)] [[PubMed](#)]
14. Zhang, D.; Jing, X.; Zhang, W.; Nie, Y.; Xu, Y. Highly Selective Synthesis of d -Amino Acids from Readily Available l -Amino Acids by a One-Pot Biocatalytic Stereoinversion Cascade. *RSC Adv.* **2019**, *9*, 29927–29935. [[CrossRef](#)] [[PubMed](#)]
15. Fan, A.; Li, J.; Yu, Y.; Zhang, D.; Nie, Y.; Xu, Y. Enzymatic Cascade Systems for D-Amino Acid Synthesis: Progress and Perspectives. *Syst. Microbiol. Biomanuf.* **2021**, *1*, 397–410. [[CrossRef](#)]
16. Park, E.-S.; Dong, J.-Y.; Shin, J.-S. Biocatalytic Asymmetric Synthesis of Unnatural Amino Acids through the Cascade Transfer of Amino Groups from Primary Amines onto Keto Acids. *ChemCatChem* **2013**, *5*, 3538–3542. [[CrossRef](#)]
17. Zhou, H.; Meng, L.; Yin, X.; Liu, Y.; Xu, G.; Wu, J.; Wu, M.; Yang, L. Artificial Biocatalytic Cascade with Three Enzymes in One Pot for Asymmetric Synthesis of Chiral Unnatural Amino Acids. *Eur. J. Org. Chem.* **2019**, *2019*, 6470–6477. [[CrossRef](#)]
18. Parmeggiani, F.; Rué Casamajo, A.; Walton, C.J.W.; Galman, J.L.; Turner, N.J.; Chica, R.A. One-Pot Biocatalytic Synthesis of Substituted D-Tryptophans from Indoles Enabled by an Engineered Aminotransferase. *ACS Catal.* **2019**, *9*, 3482–3486. [[CrossRef](#)]
19. Silva, M.V.d.M.; Costa, I.C.R.; de Souza, R.O.M.A.; Bornscheuer, U.T. Biocatalytic Cascade Reaction for the Asymmetric Synthesis of L- and D-homoalanine. *ChemCatChem* **2019**, *11*, 407–411. [[CrossRef](#)]
20. Walton, C.J.W.; Parmeggiani, F.; Barber, J.E.B.; McCann, J.L.; Turner, N.J.; Chica, R.A. Engineered Aminotransferase for the Production of D-Phenylalanine Derivatives Using Biocatalytic Cascades. *ChemCatChem* **2018**, *10*, 470–474. [[CrossRef](#)]
21. Bae, H.-S.; Lee, S.-G.; Hong, S.-P.; Kwak, M.-S.; Esaki, N.; Soda, K.; Sung, M.-H. Production of Aromatic D-Amino Acids from  $\alpha$ -Keto Acids and Ammonia by Coupling of Four Enzyme Reactions. *J. Mol. Catal. B Enzym.* **1999**, *6*, 241–247. [[CrossRef](#)]
22. Eliot, A.C.; Kirsch, J.F. Pyridoxal Phosphate Enzymes: Mechanistic, Structural, and Evolutionary Considerations. *Annu. Rev. Biochem.* **2004**, *73*, 383–415. [[CrossRef](#)] [[PubMed](#)]
23. Braunstein, A.E. 10 Amino Group Transfer. In *Enzymes*; Karger Publishers: Basel, Switzerland, 1973; pp. 379–481.
24. Bezsudnova, E.Y.; Popov, V.O.; Boyko, K.M. Structural Insight into the Substrate Specificity of PLP Fold Type IV Transaminases. *Appl. Microbiol. Biotechnol.* **2020**, *104*, 2343–2357. [[CrossRef](#)] [[PubMed](#)]
25. Tanizawa, K.; Masus, Y.; Asano, S.; Tanaka, H.; Sadas, K. Thermostable D-Amino Acid Aminotransferase from a Thermophilic *Bacillus* Species. Purification, Characterization, and Active Site Sequence Determination. *J. Biol. Chem.* **1989**, *264*, 2445–2449. [[CrossRef](#)] [[PubMed](#)]
26. Yonaha, K.; Misono, H.; Yamamoto, T.; Soda, K. D-Amino Acid Aminotransferase of *Bacillus sphaericus*. Enzymologic and Spectrometric Properties. *J. Biol. Chem.* **1975**, *250*, 6983–6989. [[CrossRef](#)]
27. Kobayashi, J.; Shimizu, Y.; Mutaguchi, Y.; Doi, K.; Ohshima, T. Characterization of D-Amino Acid Aminotransferase from *Lactobacillus salivarius*. *J. Mol. Catal. B Enzym.* **2013**, *94*, 15–22. [[CrossRef](#)]
28. Lee, S.-G.; Hong, S.-P.; Song, J.J.; Kim, S.-J.; Kwak, M.-S.; Sung, M.-H. Functional and Structural Characterization of Thermostable D-Amino Acid Aminotransferases from *Geobacillus* spp. *Appl. Environ. Microbiol.* **2006**, *72*, 1588–1594. [[CrossRef](#)]
29. Savile, C.K.; Janey, J.M.; Mundorff, E.C.; Moore, J.C.; Tam, S.; Jarvis, W.R.; Colbeck, J.C.; Krebber, A.; Fleitz, F.J.; Brands, J.; et al. Biocatalytic Asymmetric Synthesis of Chiral Amines from Ketones Applied to Sitagliptin Manufacture. *Science* **2010**, *329*, 305–309. [[CrossRef](#)] [[PubMed](#)]
30. Gu, X.; Zhao, J.; Chen, L.; Li, Y.; Yu, B.; Tian, X.; Min, Z.; Xu, S.; Gu, H.; Sun, J.; et al. Application of Transition-Metal Catalysis, Biocatalysis, and Flow Chemistry as State-of-the-Art Technologies in the Synthesis of LCZ696. *J. Org. Chem.* **2020**, *85*, 6844–6853. [[CrossRef](#)]
31. Slabu, I.; Galman, J.L.; Lloyd, R.C.; Turner, N.J. Discovery, Engineering, and Synthetic Application of Transaminase Biocatalysts. *ACS Catal.* **2017**, *7*, 8263–8284. [[CrossRef](#)]
32. Bakunova, A.K.; Nikolaeva, A.Y.; Rakitina, T.V.; Isaikina, T.Y.; Khrenova, M.G.; Boyko, K.M.; Popov, V.O.; Bezsudnova, E.Y. The Uncommon Active Site of D-Amino Acid Transaminase from *Haliscomenobacter Hydrossis*: Biochemical and Structural Insights into the New Enzyme. *Molecules* **2021**, *26*, 5053. [[CrossRef](#)]
33. Yu, X.; Bresser, J.; Schall, I.; Djurdjevic, I.; Buckel, W.; Wang, X.; Engel, P.C. Development of a Satisfactory and General Continuous Assay for Aminotransferases by Coupling with (R)-2-Hydroxyglutarate Dehydrogenase. *Anal. Biochem.* **2012**, *431*, 127–131. [[CrossRef](#)] [[PubMed](#)]
34. Chowdhury, G.; Dostalek, M.; Hsu, E.L.; Nguyen, L.P.; Stec, D.F.; Bradfield, C.A.; Guengerich, F.P. Structural Identification of Diindole Agonists of the Aryl Hydrocarbon Receptor Derived from Degradation of Indole-3-Pyruvic Acid. *Chem. Res. Toxicol.* **2009**, *22*, 1905–1912. [[CrossRef](#)] [[PubMed](#)]
35. Fuchikami, Y.; Yoshimura, T.; Gutierrez, A.; Soda, K.; Esaki, N. Construction and Properties of a Fragmentary D-Amino Acid Aminotransferase. *J. Biochem.* **1998**, *124*, 905–910. [[CrossRef](#)] [[PubMed](#)]
36. Sugio, S.; Petsko, G.A.; Manning, J.M.; Soda, K.; Ringe, D. Crystal Structure of a D-Amino Acid Aminotransferase: How the Protein Controls Stereoselectivity. *Biochemistry* **1995**, *34*, 9661–9669. [[CrossRef](#)] [[PubMed](#)]
37. Roura Padrosa, D.; Alaux, R.; Smith, P.; Dreveny, I.; López-Gallego, F.; Paradisi, F. Enhancing PLP-Binding Capacity of Class-III  $\omega$ -Transaminase by Single Residue Substitution. *Front. Bioeng. Biotechnol.* **2019**, *7*, 282. [[CrossRef](#)]

38. Börner, T.; Rämisch, S.; Reddem, E.R.; Bartsch, S.; Vogel, A.; Thunnissen, A.M.W.H.; Adlercreutz, P.; Grey, C. Explaining Operational Instability of Amine Transaminases: Substrate-Induced Inactivation Mechanism and Influence of Quaternary Structure on Enzyme-Cofactor Intermediate Stability. *ACS Catal.* **2017**, *7*, 1259–1269. [[CrossRef](#)]
39. Pavkov-Keller, T.; Strohmeier, G.A.; Diepold, M.; Peeters, W.; Smeets, N.; Schürmann, M.; Gruber, K.; Schwab, H.; Steiner, K. Discovery and Structural Characterisation of New Fold Type IV-Transaminases Exemplify the Diversity of This Enzyme Fold. *Sci. Rep.* **2016**, *6*, 38183. [[CrossRef](#)]